Ceramics International 22 (1996) 471–475

0272-8842/96 $15.00+.00
0272-8842(95)00111-5

Phase Diagram of Oxygen Ordering in High Temperature Superconductor $YBa_2Cu_3O_x$

S. G. Titova, S. G. Sludnov, V. F. Balakirev, O. M. Fyodorova, T. I. Arbuzova & O. V. Morozova

Institute of Metallurgy, Ural Division of Russian Academy of Sciences, Amundsen St. 101, Ekaterinburg 620016, Russia

(Received 9 December 1994; accepted 10 May 1995)

Abstract: In order to investigate the phase diagram of oxygen ordering in $YBa_2Cu_3O_x$, structural, magnetic and thermogravimetric measurements were carried out. Calculations for intercalated system with quasi-elastic interaction between inserted oxygen and host lattice are presented. © 1996 Elsevier Science Limited and Techna S.r.l.

1 INTRODUCTION

Numerous papers[1–24] report experimental results[1–7] and calculations[8–23] of phase transition behaviour of $YBa_2Cu_3O_x$ over wide temperature ranges. The tetragonal (T) to orthorhombic (OR) phase boundary is readily located directly, by X-ray diffraction, or indirectly, from thermodynamic functions obtained by oxygen vapour pressure measurements. The locations differ, depending on determination of the oxygen content by different authors.[3,7]

Parfionov and Chernyshov,[4] by thermogravimetric measurements in helium atmosphere, have obtained a concentration dependence of oxygen chemical potential with two steps which the authors explain as arising from T–ORII and ORII–ORI phase transitions. They observed a triple-point with coordinates: $T = 740 + 5$ K, $x = 6.63 + 0.03$. The T–ORII transition was attributed to the appearance of another type of hole electronic carriers with high mobility and the ORII–ORI transition to the increasing concentration of these hole carriers.[5]

We replotted experimental data of temperature dependence of thermoelectrical power $S(T)$ for $YBa_2Cu_3O_x$ with different oxygen content;[25] that is a function of $S(x)$ (Fig. 1). Rapid change of $S(x)$ with sign inversion takes place near $x = 6.70$–6.73 for the temperature range 100–300 K.

In Fig. 2 we present the concentration dependence of dc-magnetic susceptibility obtained from temperature dependences.[26,27] Inspection of the figure shows that there are three areas of susceptibility with discontinuities at $x = 6.25$–6.35 and $x = 6.60$–6.70 which are associated with T–ORII and ORII–ORI boundaries. These boundaries have very small deviation, being almost parallel to the T-axes at low temperatures in this interpretation.

There are also many papers[1,28–31] where authors observe anomalies of internal friction and elastic modulii at 100–110, 140–160, 230 and 280–310 K by ultrasonic measurements. The anomaly in the 140–160 K temperature range disappears as oxygen content is decreased; it can be related to twinning.[1,29]

The anomaly near 230 K has an "order–disorder" character;[30,31] some authors connect it with ORI–ORII or ORI–(ORI + ORII) transitions.[1,32,33] We have reported[33] some properties of the ORII-phase (diffraction diffuse maximum for $2 * a$ superstructure, contribution of separated spin and charge Cu–O states of planes and chains to magnetic susceptibility) observed for a sample with oxygen content $x = 6.96$ below 230 K. Naish *et al.*[34] observed the same small diffraction diffuse

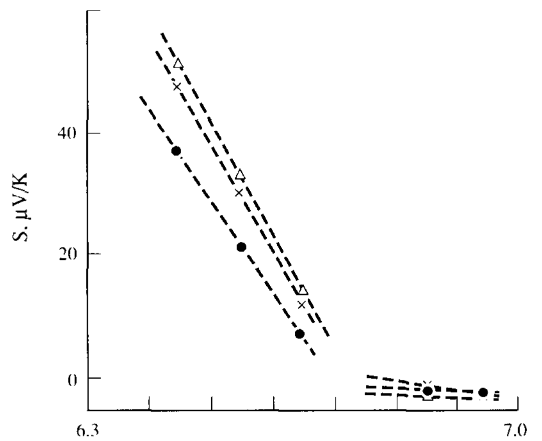

Fig. 1. Thermoelectric power $S(x)$ as a function of oxygen content, replotted from temperature dependences[25–27] at temperatures △ — 160 K, x — 200 K, ● — 300 K. Dashed lines are the measurements of Nakazawa and Ishikawa,[27] dot-and-dash lines are the results of Samokhvalov *et al.*[26]

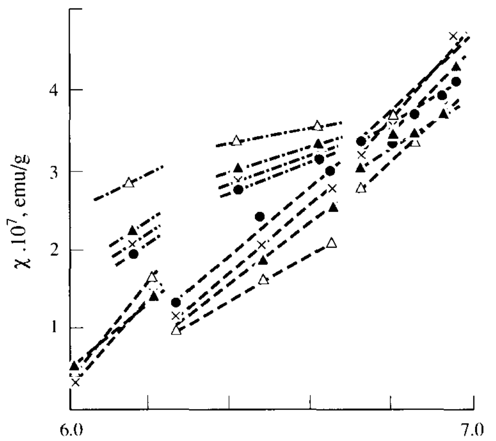

Fig. 2. dc-magnetic susceptibility $\chi(x)$ as a function of oxygen content, replotted from temperature dependences[25–27] at temperatures △ — 160 K, x — 200 K, ▲ — 250 K, ● — 300 K. Dashed lines are the measurements of Nakazawa and Ishikawa,[27] dot-and-dash lines are the results of Samokhvalov *et al.*[26]

maximum for the $2 * a$ superstructure for a single crystal with $x = 7$ at room temperature and discussed their results in terms of a model having anomalous thermal factors for Cu1 and O4 atoms.

There are also many reports about different types of superstructure,[35] for example 1/3 ($3 * a$, ORIII-phase), 5/2 and others with general formula $Y_8Ba_{16}Cu_{24}O_{56-m}$ ($0 < m < 8$, m even) observed using high resolution electron microscopy.[36] These compounds can be considered as members of a family of phases in which one of every n (n = 1,2,3...) oxygen chains are missing from the basal plane of the unit cell.[23,24]

In most theoretical papers where phase transitions in $YBa_2Cu_3O_x$ have been investigated, oxygen ordering in the basal plane is evaluated using a model with anisotropic interaction between nearest and next-nearest neighbours (ASYNNI-model).[8–10,12] In this model, the T-phase and ORI-phase are considered as disordered with arbitrary occupation of sublattices 1 and 2 (O4 and O5 sites). The T–OR transition is accompanied by separation of oxygen and vacancies into sublattices 1 and 2, respectively.

Because a two-dimensional model cannot be applied exactly when constructing phase diagrams, different approximative methods are used: Monte Carlo simulations,[19,20] lattice-gas model by cluster-variation method,[11,15–18] etc. Accounting for interactions between more remote neighbours (also in c-direction) leads to a more realistic form of the phase diagram.[17,21,22,32]

In Section 2 we will show X-ray diffraction and dc-magnetic susceptibility measurements at 77–300 K; thermogravimetric data at 50–1000°C have been used for phase transition investigation of $YBa_2Cu_3O_x$ with different oxygen content.

In Section 3 we will present our calculated phase diagram by using the Dahn, Dahn and Haering (DDH) model[37] for oxygen ordering in $YBa_2Cu_3O_x$, considered as an intercalated system.

Table 1. The thermal treatment and characterisation of $YBa_2Cu_3O_x$ samples

Sample	Temperature of exposure (°C)	Unit cell parameters			Oxygen content		
		a	*b* (nm)	*c*	From TGA data	From Ref. 5	From Ref. 38
1	550	0.3828	0.3893	1.1660	6.96	7.00	6.96
2	580	0.3833	0.3893	1.1671	6.90	6.95	6.85
3	600	0.3836	0.3892	1.1675	6.80	6.85	6.80
4	650	0.3836	0.3891	1.1677	6.78	6.83	6.78
5	680	0.3837	0.3885	1.1686	6.67	6.78	6.70
6	730	0.3842	0.3873	1.1693	6.65	6.70	6.63
7	830	0.3846	0.3856	1.1694	6.60	6.60	6.61
8	930	0.3856	0.3856	1.1848	6.35	6.35	6.20

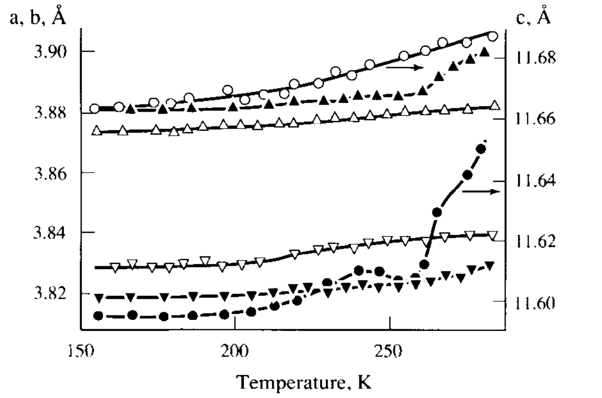

Fig. 3. Unit cell parameters for $YBa_2Cu_3O_x$ with $x = 6.60$ (open symbols) and $x = 6.96$ (filled symbols) as functions of temperature: ▽, ▼ — *a*-axis; △, ▲ — *b*-axis; ○, ● — c-axis, respectively.

2 EXPERIMENTAL RESULTS

Ceramic samples of $YBa_2Cu_3O_x$ with a density of 5.7–5.8 g/cm^3 are produced with traditional solid state synthesis from high purity initial reagents. The initial composition ($YBa_2Cu_3O_7$) was produced by annealing in oxygen atmosphere for 6–8 h at 500°C. Thermal exposures (6–8 h) at appropriate temperatures[29] have been used to remove oxygen (see Table 1). The oxygen content of the samples was measured by the weight change of the sample by thermogravimetry (TGA). We proceeded from the supposition that the endo-effect at 930°C corresponds to $x = 6.25$. The accuracy of the oxygen content determination was equal to $x = \pm 0.05$. In Table 1 the oxygen content determined from the concentration dependence of unit cell parameters according to Refs 5 and 38 is shown for comparison.

Structural investigations were carried out on the DRON-1UM X-ray diffractometer (CuK_α, Ni-filtered) in helium atmosphere. The lattice parameters determined from a least squares fitting to about 15 diffraction line positions are shown as a function of temperature (Fig. 3). The standard deviation for an individual measurement is 0.013.

Magnetic susceptibility has been measured by the Faraday method at a field of 9 kOe (Fig. 4).

From Fig. 3 we see that both samples with $x = 6.96$ and $x = 6.60$ ($N = 1$ and $N = 7$ from Table 1) have structural anomalies near 230 K, with increased thermal expansion coefficients, but the more oxygen-rich sample demonstrates more complex behaviour of unit cell parameters with a maximum and minimum in this temperature range.

Magnetic susceptibility has a temperature independent Pauli-like behaviour above 230 K and a "Curie–Weiss" contribution below 230 K for the sample with $x = 6.96$ ($N = 1$ from Table 1). For sample $x = 6.90$ ($N = 2$) this "Curie–Weiss" term appears below 290 K and has a small step at 230 K. So at 230 K we have observed transitions occurring both in the ORI and ORII phases, related to effects of antiferromagnetic type localisation (with negative values of the Curie–Weiss constant Θ).

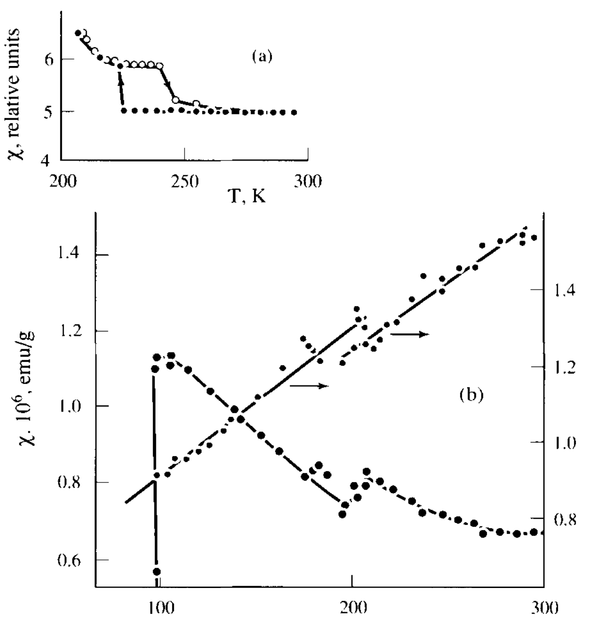

Fig. 4. Magnetic susceptibility as a function of temperature for $YBa_2Cu_3O_x$: (a) with oxygen content $x = 6.96$; (b) $x = 6.60$.

Assuming that the "Curie–Weiss" term in the susceptibility for samples with $x > 6.8$ is conditioned by the ORII-phase contribution, we attempted to find the (ORI + OTII)–ORI boundary using thermogravimetry. Except for two small endothermic effects at 220–240°C and 440°C, nothing was observed. The first effect has its maximum value for concentration $x = 6.8$–6.9 and is connected with small extraction of oxygen from the sample, whereas the second is greatest for $x = 6.0$–6.7; it is connected with insertion of oxygen into the sample. Both of these effects are related to exchange of oxygen between ORI–ORII clusters because of differences in oxygen chemical potentials between them.

The absence of a plateau on the concentration dependence of unit cell parameters for $YBa_2Cu_3O_x$, both at room temperature and at high temperatures,[5,38,39] could indicate the absence of phase mixtures (ORI + ORII).

3 CALCULATIONS

For intercalated compounds, Safran[40] suggested a model describing phase diagrams with a Hamiltonian:

$$H = -\mu \sum i\, \sigma_i + \frac{1}{2} U_0 \sum j\, \sigma_j^2 - \frac{1}{2} \sum ij\, V_{ij}\sigma_i\sigma_j,$$

where i is the number of the row, $U_o > 0$ and $V_{ij} > 0$ are the energy of interaction of inserted ions within and between the rows, μ is the chemical potential, and σ is the concentration of inserted ions in the row.

This Hamiltonian was completed by the term of quasi-elastic interaction between intercalated ions and host lattice:[37]

$$U(\sigma) = J\sigma/(\alpha + \sigma),$$

where α is the constant of quasi-elastic interaction, and $J \sim 0.7$ eV. It was shown[41] that the DDH model can be successfully used for quantitative description for a real system with inserted atoms.

Using a mean field approximation we find a free energy minimum as a function of oxygen concentration, with chemical potential as the parameter. Experimental results[6,7] were used for obtaining chemical potential as a function of oxygen content. A quasi-elastic constant, α, was obtained from the concentration dependence of the cell parameters.[5,38]

We suggest that the entropy depends only on the concentration of oxygen in the row and is not connected with occupation of the other rows.

The $YBa_2Cu_3O_x$ phase diagram, computed with a model accounting for interactions up to 4 chains, is shown in Fig. 5 for interaction parameters $U_o = 0.01$, $V_{i,i+1} = 0.8$, $V_{j,j+2} = 0.1$, $\alpha = 0.4$, where U_o, $V_{i,i+1}$, $V_{j,j+2}$ are parameters of interaction within the row, between nearest rows and between next-nearest rows, respectively.

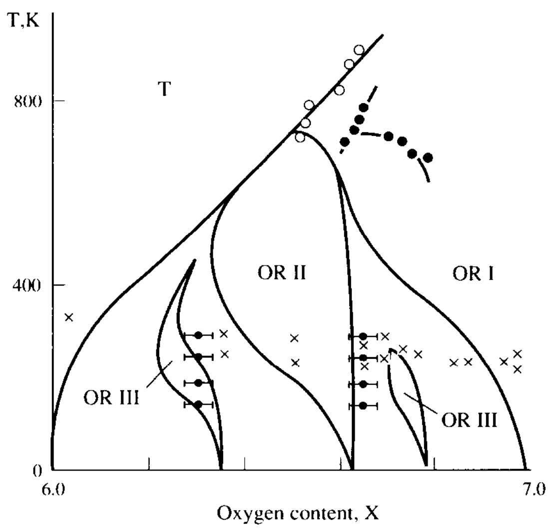

Fig. 5. Pseudo-binary phase diagram as computed with the DDH model[37] ($U_o = 0.01$, $V_{i,i+1} = 0.8$, $V_{j,j+2} = 0.1$, $\alpha = 0.4$). Filled and open circles are experimentally measured transition points.[4,6] x — experimental points of internal friction anomalies[28,2930,31] in the temperature range 200–320 K at a frequency of 60–90 kHz. T–ORII and ORII–ORI boundaries obtained from thermoelectric power and dc-magnetic susceptibility measurements (see Figs 1 and 2) are shown as points.

Main features of our calculated phase diagram are the:

1. presence of a T-point, above which the ORI–ORII boundary becomes a second order phase transition without phase mixing;
2. presence of more high stage ORIII-phase which vanishes at negative values of the U_o and $V_{i,i+2}$ parameters;
3. width of ordering stage regions ORII, ORIII which decrease as the temperature decreases;
4. decreasing quasi-elastic interaction constant, leading to the disappearance of the triple-point.

4 SUMMARY

According to diffraction and magnetic data (Figs 2–4), we can conclude that the phase transition lines of T–ORII and ORII–ORI are almost parallel to the T-axis at low temperature. These features are in our calculated diagram (Fig. 5). From this figure one can see that the model developed here, with quasi-elastic interactions between lattice and inserted atoms, is suitable for the description of the phase diagram of $YBa_2Cu_3O_x$ with oxygen ordering.

In spite of the fact that in our model the transition ORI–ORII is first order at low temperature, the phase mixture (ORI + ORII) can not be founded by experimental methods: concentration dependences of critical temperature and unit cell parameters[38] have a significant change upon increasing the oxygen content from 6.8 to 7.0. But the observed contribution of the ORII-phase to the properties of compounds with $x = 6.8$–6.96 (magnetic and diffraction data,[26,27] Fig. 4) can be connected to the microscopic mixture of ORII-cells in the ORI-lattice. For example, critical temperature concentration dependence was described in the model of the ORI and ORII micromixture.[42]

We suggest that discrepancies between calculations and experimental results can be related to the occurrence of metastable states.

REFERENCES

1. TOKMAKOVA, S. P. & CHABAN, I. A., *Superconductivity: Physics, Chemistry, Technology (Russ.)*, **11** (1990) 2567.

2. PIETRASZKO, A., WOLCYRZ, M., HORYN, R., BUKOWSKI, Z., LUKASZEWICZ, K. & KLAMUT, J., *Cryst. Res. Technol.*, **23**(3) (1988) 351.
3. PARFIONOV, O. E. & CHERNYSHOV, A. A., *Superconductivity: Physics, Chemistry, Technology (Russ.)*, **6** (1989) 5.
4. PARFIONOV, O. E. & CHERNYSHOV, A. A., *Superconductivity: Physics, Chemistry, Technology (Russ.)*, **3** (1990) 512.
5. PARFIONOV, O. E., *Superconductivity: Physics, Chemistry, Technology (Russ.)*, **2** (1992) 319.
6. SCHLEGER, P., HARDY, W. W. & YANG, B. X., *Physica C*, **176** (1991) 261.
7. LOKHTIN, A. A., LEONIDOV, I. A. & TSIDILKOVSKI, V. I., *Superconductivity: Physics, Chemistry, Technology (Russ.)*, **4** (1992) 185.
8. de FONTAINE, D., WILLE, L. T. & MOSS, S. C., *Phys. Rev.*, **B36**(10) (1987) 5709.
9. WILLE, L. T., BARERA, A. & de FONTAINE, D., *Phys. Rev. Lett.*, **60**(11) (1988) 1065.
10. WILLE, L. T., *Phys. Rev.*, **B40**(10) (1989) 6931.
11. BARERA, A. & de FONTAINE, D., *Phys. Rev.*, **B39**(10) (1989) 6727.
12. CEDER, G., ASTA, M. & de FONTAINE, D., *Physica C*, **177** (1991) 106.
13. KHANNA, R., WELBERRY, T. R. & ANANTHAKRISHNA, G., *Physica C*, **197** (1992) 57.
14. KIKUCHI, R. & CHOI, J.-S., *Physica C*, **160** (1989) 347.
15. ZUBKUS, V. E., LAPINSKAS, S. & TORNAU, E. E., *Phys. Stat. Solid (b)*, **156**(1) (1989) 93.
16. ZUBKUS, V. E., LAPINSKAS, S. & TORNAU, E. E., *Physica C*, **159** (1989) 501.
17. ZUBKUS, V. E., TORNAU, E. E., LAPINSKAS, S. & KUNDROTAS, P. J., *Phys. Rev.*, **B43**(16) (1991) 13112.
18. ZUBKUS, V. E., PARFIONOV, O. E., TORNAU, E. E. & KUNDROTAS, P. J., *Physica C*, **198** (1992) 141.
19. ZHI-XIONG, C. & MAHANTI, S. D., *Phys. Rev.*, **B40**(10) (1989) 6558.
20. AUKRUST, T., NOVOTNY, M. A., RIKVOLD, P. A. & LANDAU, D. P., *Phys. Rev.*, **B41**(13) (1990) 8772.
21. KHACHATURYAN, A. G. & MORRIS, J. W., *Phys. Rev. Lett.*, **59**(24) (1987) 2776.
22. KHACHATURYAN, A. G., SEMENOVSKAYA, S. V. & MORRIS, J. W., *Phys. Rev.*, **B37**(4) (1988) 2243.
23. KHACHATURYAN, A. G. & MORRIS, J. W., *Phys. Rev. Lett.*, **61**(2) (1988) 215.
24. GOODENOUGH, J. B., *J. Mater. Edu.*, **9**(6) (1987) 619.
25. KRYLOV, K. R., PONOMAREV, A. I., TSIDILKOVSKI, I. M., TSIDILKOVSKI, V. I., BASUEV, G. V., KOSHEVNIKOV, I. L. & CHESHNITSKI, S. M., *Phys. Lett.*, **A131**(3) (1988) 203.
26. SAMOKHVALOV, A. A., CHEBOTAEV, N. M., KOSTYLEV, V. A., GIZCHEVSKI, B. A., ARBUZOVA, T. I., VATOLIN, N. A. & NAUMOV, S. V., *PhMM (Russ.)*, **67**(4) (1989) 741.
27. NAKAZAWA, Y. & ISHIKAWA, M., *Physica C*, **158** (1989) 381.
28. GUSAKOVSKAYA, I. G., PIRUMOVA, S. I. & ATOVMYN, L. O., *Superconductivity: Physics, Chemistry, Technology (Russ.)*, **3**(9) (1990) 1980.
29. PAL-VAL, P. P., PAL-VAL, L. N., DEMIRSKII, V. D., NATSIK, V. D. & PRYTKIN, V. V., *Superconductivity: Physics, Chemistry, Technology (Russ.)*, **4**(8) (1991) 1542.
30. NATSIK, V. D., PAL-VAL, P. P., ENGERT, J. & KAUFMANN, Ch.-J, *Phys. of Low Temp. (Ukr.)*, **15**(8) (1989) 836.
31. NATSIK, V. D., PAL-VAL, P. P., ENGERT, J., KAUFMANN, Ch.-J., RUDOLF, K. & MATZ, V., *Phys. of Low Temp. (Ukr.)*, **16**(3) (1990) 293.
32. CHYSHAK, Y. G. & GURSKII, Z. A., *Superconductivity: Physics, Chemistry, Technology (Russ.)*, **4**(11) (1991) 2119.
33. TITOVA, S. G., FOTIEV, V. A., PASCHENKO, A. V., BURKHANOV, A. M., GUDKOV, V. V., ZCHEVSTOVSKIKH, I. V., TKACH, A. V. & USTINOV, V. V., *Superconductivity: Physics, Chemistry, Technology (Russ.)*, **4**(5) (1991) 1010.
34. KASSAN-OGLY, Ph.A., NAISH, V. E. & SAGARADZE, T. V., *Superconductivity: Physics, Chemistry, Technology (Russ.)*, **3**(5) (1990) 825.
35. WERDER, D. J., CHEN, C. H., CAVA, R. J. & BATLOGG, B., *Phys. Rev.*, **B37**(4) (1988) 2317.
36. ALARIO-FRANCO, M. A., CHAILLOUT, C., CAPPONI, J. J., CHENEVAS, J. & MAREZIO, M., *J. Less-Common Metals*, **150** (1989) 117.
37. DAHN, J. R., DAHN, D. C. & HAERING, R. R., *Solid State Commun.*, **42**(3) (1982) 179.
38. CAVA, R. J., HEWAT, A. W., HEWAT, E. A., BATLOGG, B., MAREZIO, M., RABE, K. M., KRAJEWSKI, J. J., PECK, W. F. Jr & RUPP, L. W., *Physica C*, **165** (1990) 419.
39. TOUZELIN, B. & MARUCCO, J. F., *J. Less-Common Metals*, **144** (1988) 283.
40. SAFRAN, S. A., *Phys. Rev. Lett.*, **44**(14) (1980) 937.
41. TITOV, A. N. & BIKKIN, Ch.M., *Phys. of Solid States (Russ.)*, **33**(6) (1991) 1876.
42. POULSEN, H. F., ANDERSEN, N. H., ANDERSEN, J. V., BOHR, H. & MOURITSEN, O. G., *Lett. to Nature*, **349**(6310) (1991) 594.